# NUMERICAL ANALYSIS OF TRANSIENT CONVECTION HEAT TRANSFER EMPLOYING TWO DIFFERENT TEMPORAL SCHEMES: EXPLICIT ITERATIVE OF TAYLOR-GALERKIN AND TWO STEP EXPLICIT

**Elizaldo Domingues dos Santos, edsantos@mecanica.ufrgs.br**
**Guilherme Luiz Piccoli, glpiccoli@mecanica.ufrgs.br**
**Francis Henrique Ramos França, frfranca@mecanica.ufrgs.br**
**Adriane Prisco Petry, adrianep@mecanica.ufrgs.br**
Department of Mechanical Engineering
Universidade Federal do Rio Grande do Sul – Rua Sarmento Leite, 425 – Porto Alegre - RS

***Abstract.*** *The present work studies two different approaches of time integration in order to investigate the hydrodynamic and thermal behavior of transient internal flows with mixed convection heat transfer. The two temporal schemes are: Explicit Iterative of Taylor-Galerkin (EITG) and Two Step Explicit (TSE). The conservation equations of mass, momentum and energy are solved by three-dimensional codes developed using the Finite Element Method (FEM) with eight-node hexahedral element. A two-dimensional mixed convection problem of cavity flow in the laminar regime is simulated, with Reynolds number of Re=400, Prandtl number of Pr=6, and Richardson number of Ri=0.1. The velocities and temperature fields obtained from the two different approaches are compared, showing satisfactory results when confronted with literature; the results agreed within 6%. Moreover, the processing times obtained from the two approaches are compared: the TSE method required a CPU time around 8 times lower than the EITG method. The reduction of time processing allows simulations in three-dimensional flows, which is important in the prediction of some hydrodynamics and thermal structures, e.g., Taylor-Göertler vortexes. In order to capture such structures, the same 2D simulation is performed in a three-dimensional domain.*

***Keywords****: Mixed convection, Transient Flows, Explicit Iterative Scheme, Two Step Explicit Scheme*

## 1. INTRODUCTION

Numerical analyses of mixed convection heat transfer transient flows in many engineering equipments and thermal devices, e.g., heat exchangers, combustion chambers, turbines and others, have increased substantially. However, they still demand a high computational effort. Some reasons for this are the non-linear behavior of these flows and its multiple interactive scales. For instance, according to Wang *et al.* (2005), the set of equations to be simultaneously solved for the estimative of all scales of mixed convection flows is in the order of $Pr^3Re^{9/4}$, which still limits its application to simple geometries with low Reynolds numbers. Therefore, parallel computation techniques, high-performance programming and different methods of spatial and temporal discretization are studied with the purpose of reducing the computational costs linked to the numerical simulation of complex mixed convection flows. The first and second ones will not be addressed in the present work, since they were previously studied by Piccoli *et al.* (2008).

Concerning the temporal numerical integration schemes, the implicit ones are unconditionally stable and the time increment can be taken longer than that of the explicit schemes. In contrast, the implicit schemes require a large size of computer core storage, increasing significantly the processing time. On the other hand, when the explicit scheme is used, the computer core storage can be drastically reduced (Kawahara and Hirano, 1983). Furthermore, when turbulent flows are simulated, the time step is conditioned by the high frequencies of the small scales, so substantially short time increments are required. In this sense, the explicit schemes are more often used than the implicit ones (Petry and Awruch, 2006).

One difficult in the application of the explicit schemes is in the simulation of incompressible flows. This is due to temporal independence of derivative of pressure in the continuity equation, which generates zero values in the diagonal terms of mass matrix. Thereby, the conditioning of the simultaneous equation system is drastically reduced. Nevertheless, this difficult can be overcome by the employment of some methods as penalty function, solution of Poisson equation and pseudo-compressibility that have been proposed in the literature (Kawahara and Hirano, 1983; Reddy and Gartling, 1994; Zienkiewicz and Taylor, 2000). In the present work the Explicit Iterative of Taylor-Galerkin (EITG) and the Two Step Explicit (TSE) temporal schemes are employed in the transient simulations. Both schemes have been used in simulations of isothermal flows (Braun and Awruch, 2003; Petry, 1993; Petry and Awruch, 2006; Teixeira and Awruch, 2001) and non-isothermal flows (Dos Santos *et al.*, 2007; Popiolek *et al.*, 2006).

In the present work, the conservation equation of mass, which is modified from the pseudo-compressibility method (Chorin, 1967; Kawahara and Hirano, 1983), momentum and energy in the transient regime are solved by the finite element method (FEM) with eight-node isoparametric hexahedral element, using spatial discretization of Bubnov-Galerkin and reduced integration of element matrices. In order to evaluate the prediction of fluid dynamic and thermal behavior from the two mentioned schemes (EITG and TSE) the simulation of transient, two-dimensional, non-

isothermal flows in cavities are presented for Reynolds number of $Re_H = 400$, Prandtl number of $Pr = 6$ and Richardson number of $Ri = 0.1$. The transient velocity and temperature fields obtained in this work are compared to those presented in Ji *et al.* (2007). Time processing obtained from the two temporal schemes is also computed with the purpose to evaluate the most suitable scheme in the simulation of more complex flows, e.g., three-dimensional and turbulent flows. The literature has presented some investigations about two-dimensional mixed convection transient flows (Ji *et al.*, 2007), and a few three-dimensional mixed convection flows at the steady state (Iwatsu and Hyun, 1995). However, little has been presented for the investigation of thermal structures in three-dimensional mixed convection transient flows, even in the laminar regime. In order to perform this investigation, the temporal scheme that requires the lowest computational effort will be employed in the simulation of transient, non-isothermal, laminar, three-dimensional flow. The same dimensionless parameters of the 2D simulation are used in the 3D simulation, $Re_H = 400$, $Pr = 6$ e $Ri = 0.1$.

## 2. MATHEMATICAL MODELING

The modeling of transient, non-isothermal flows is based on the solution of conservation equations together with the boundary and the initial conditions. After the employment of pseudo-compressibility approach (Kawahara and Hirano, 1983) the conservation equations modified of mass, momentum and energy, valid in an orthonormal basis, are given by:

$$\frac{\partial P}{\partial t} + v_j \frac{\partial P}{\partial x_j} + C^2 \frac{\partial}{\partial x_j}\left(\rho v_j\right) = 0 \qquad (j = 1, 2 \text{ and } 3) \text{ in } t \times \Omega \tag{1}$$

$$\frac{\partial}{\partial t}\left(\rho v_i\right) + \frac{\partial}{\partial x_j}\left(\rho v_i v_j\right) + \frac{\partial P}{\partial x_j}\delta_{ij} - \frac{\partial}{\partial x_j}\left\{\rho \upsilon\left(\frac{\partial v_i}{\partial x_j} + \frac{\partial v_j}{\partial x_i}\right) + \lambda \frac{\partial v_k}{\partial x_k}\right\} + \rho g_i \beta\left(T - T_0\right) = 0 \quad (i, j, k = 1,2 \text{ and } 3) \text{ in } t \times \Omega \tag{2}$$

$$\frac{\partial T}{\partial t} + \frac{\partial}{\partial x_j}\left(v_j T\right) - \frac{\partial}{\partial x_j}\left\{\alpha \frac{\partial T}{\partial x_j}\right\} - q''' = 0 \qquad (j = 1,2 \text{ and } 3) \text{ in } t \times \Omega \tag{3}$$

where $\rho$ is the specific mass of the fluid (kg/m³); $\beta$ is the thermal expansion coefficient ($K^{-1}$); $C$ is the sound propagation speed (m/s); $\mu$ is the dynamic viscosity (kg/ms); $\lambda$ is the volumetric viscosity (kg/ms); $\upsilon$ is the kinematic viscosity (m²/s); $\alpha$ is the thermal diffusivity (m²/s); $v_i$ is the velocity in $i$-direction, $i$ = 1, 2 and 3 (m/s); $x_i$ corresponds to the spatial coordinate, $i$ = 1, 2 and 3 (m); $P$ is the pressure (N/m²); $T$ is the temperature (°C or K); $T_0$ is the reference temperature (°C or K); $g_i$ is the gravity acceleration in $i$-direction, $i$ = 1, 2 and 3 (m/s²); $\delta_{ij}$ is the Kronecker delta; $\Omega$ is the spatial domain (m); $t$ represents the time domain (s) and $q'''$ is the heat source term (W/m³).

## 3. NUMERICAL MODELING

The finite element method (FEM) with eight-node isoparametric hexahedral element is employed in the numerical solution of the conservation equations that model two- and three-dimensional heat transfer in cavities. The Galerkin method is employed for the spatial discretization and reduced integration of element matrices (Reddy and Gartling, 1994; Zienkiewicz and Taylor, 2000). In the present work the sole interest is the study of temporal discretization.

### 3.1. Explicit Iterative of Taylor-Galerkin Scheme (EITG)

For simplification, it is presented here only the construction of the algorithm employed in the simulation of non-isothermal transient flows with EITG temporal scheme. Further detailed information can be found in Dos Santos (2007). The algorithm may be summarized in the following steps:

(1) Initiate the time step: $t + \Delta t$;

(2) Form vectors $\{S_i\}$, $\{T_C\}$ and $\{S_T\}$, Eq. (4)-(6), referent to the conservation equations of momentum, mass and energy, respectively. These vectors are independent of the iterative process:

$$\{S_i\} = -\Delta t\left\{\mathbf{A}_{ij}\left(v_i\right) + \mathbf{D}_{ij}\left(v_j\right) - \mathbf{G}_i P - \frac{1}{2}\left(\mathbf{F}_i - \mathbf{B}_i T\right)\right\}^n \qquad (i,j = 1,2 \text{ and } 3) \tag{4}$$

$$\{T_C\} = -\Delta t \mathbf{G}_j^T \left(v_j\right)^n \qquad (j = 1,2 \text{ and } 3) \tag{5}$$

$$\{S_T\} = -\Delta t\left\{\mathbf{A}_{jT}\left(T\right) + \mathbf{D}_{jT}\left(T\right) - \frac{1}{2}\mathbf{F}_T\right\}^n \qquad (j = 1,2 \text{ and } 3) \tag{6}$$

(3) Initiate the iterative process: $k = k + 1$;

(4) Form the vectors $\{R_i\}$, $\{Q\}$ and $\{R_T\}$, Eq. (7)-(9), related with conservation equations of momentum, mass and energy, respectively. These vectors are dependent of iterative process and they are obtained as function of the variation of primary variables:

$$\{R_i\} = -\frac{\Delta t}{2}\left\{\mathbf{A}_j(\Delta v_i) + \mathbf{D}_{ij}(\Delta v_j) - \frac{1}{2}(\Delta \mathbf{F}_i - \mathbf{B}_i \Delta T) + \frac{2}{\Delta t}(\mathbf{M}_V - \mathbf{M}_{DV})\Delta v_i\right\}_k^{n+1} \qquad (i,j = 1,2 \text{ and } 3) \tag{7}$$

$$\{Q\} = -\frac{\Delta t}{2}\mathbf{G}_j^T(\Delta v_j)_k^{n+1} - (\mathbf{M}_P - \mathbf{M}_{DP})(\Delta P)_k^{n+1} \qquad (j = 1,2 \text{ and } 3) \tag{8}$$

$$\{R_T\} = -\frac{\Delta t}{2}\left\{\mathbf{A}_{jT}(\Delta T) + \mathbf{D}_{jT}(\Delta T) - \frac{1}{2}\Delta \mathbf{F}_T + \frac{2}{\Delta t}(\mathbf{M}_T - \mathbf{M}_{DT})\Delta T\right\}_k^{n+1} \qquad (j = 1,2 \text{ and } 3) \tag{9}$$

(5) Calculate the temporal variation of velocity, pressure and temperature fields, Eq. (10)-(12), respectively:

$$(\Delta v_i)_{k+1}^{n+1} = \mathbf{M}_{DV}^{-1}\left[\{S_i\}^n + \{R_i\}_k^{n+1}\right] \qquad (i = 1,2 \text{ and } 3) \tag{10}$$

$$(\Delta P)_{k+1}^{n+1} = \mathbf{M}_{DP}^{-1}\left[\{T\}^n + \{Q\}_k^{n+1}\right] \tag{11}$$

$$(\Delta T)_{k+1}^{n+1} = \mathbf{M}_{DT}^{-1}\left[\{S_T\}^n + \{R_T\}_k^{n+1}\right] \tag{12}$$

(6) Impose the boundary conditions to the variation of variables in Eqs. (10)-(12);

(7) Verify if the variation of primary variables, at each iterative step, establish the specified convergence criteria. Case the convergence is established the algorithm proceeds to next step, otherwise, it returns to step (3);

(8) Update of velocity, pressure and temperature fields at each time step from the following expressions: $v_i^{n+1} = v_i^{n+1} + (\Delta v_i)_k^{n+1}$, $P^{n+1} = P^n + (\Delta P)_k^{n+1}$ and $T^{n+1} = T^n + (\Delta T)_k^{n+1}$.

(9) Impose the boundary conditions of primary variables;

(10) If the final time established for the simulation is reached the algorithm is finished, otherwise, it returns to step (1);

In the above equations, Eqs. (4)-(12), $\mathbf{M}_{DP}$, $\mathbf{M}_{DV}$ and $\mathbf{M}_{DT}$ are the discrete matrices for pressure, velocity and temperature, respectively; $\mathbf{M}_P$, $\mathbf{M}_V$ and $\mathbf{M}_T$ are the consistent matrices for pressure, velocity and temperature, respectively; $\mathbf{A}_j$ and $\mathbf{A}_{jT}$ are the advective matrices for momentum and energy; $\mathbf{D}_{ij}$ and $\mathbf{D}_{jT}$ are the diffusion matrices for momentum and energy; $\mathbf{G}_j^T$ is the matrix that carries the velocity divergent terms; $\mathbf{G}_i$ is the matrix of pressure gradients; $\mathbf{F}_i$ is the matrix that contains the buoyancy force terms as a function of the reference temperature and the Neumann boundary conditions (surface forces); $\mathbf{B}_i$ is the matrix that carries the force terms that are dependent of the temperature field; and finally, the matrix $\mathbf{F}_T$ contains the terms of volumetric heat generation and the Neumann boundary conditions (prescribed fluxes). The superscripts $(n)$ and $(n+1)$ are related to the time steps in $(t)$ and $(t + \Delta t)$, and the superscript $(k)$ indicates the iterative steps.

### 3.2. Two Step Explicit Scheme (TSE)

As with the previous scheme, it is presented here only the steps that are necessary to construct the algorithm employed in the simulation of non-isothermal flows with TSE temporal scheme. Further explanation about the scheme can be found in Braun (2007), Kawahara and Hirano (1983) and Petry (1993).

The algorithm can be summarized in the following steps:

(1) Initiate the time step: $t + \Delta t$;

(2) Form the vectors $\{S_i\}$, $\{T_C\}$ and $\{S_T\}$, Eqs. (13)-(15), related to the conservation equations of momentum, mass and energy in the first time step:

$$\{S_i\} = \frac{\Delta t}{2}\left\{\mathbf{A}_j(v_i) + \mathbf{D}_{ij}(v_j) - \mathbf{G}_i P + (\mathbf{B}_i T - \mathbf{F}_i)\right\}^n \qquad (i,j = 1,2 \text{ and } 3) \tag{13}$$

$$\{T_C\} = \frac{\Delta t}{2}\left\{\mathbf{G}_j^T(v_j) + \mathbf{K}_j(P)\right\}^n \qquad (j = 1,2 \text{ and } 3) \tag{14}$$

$$\{S_T\} = \frac{\Delta t}{2}\left\{\mathbf{A}_{jT}(T) + \mathbf{D}_{jT}(T) - \mathbf{F}_T\right\}^n \qquad (j = 1,2 \text{ and } 3) \tag{15}$$

(3) Calculate the velocity ($v_i^{n+1/2}$), pressure ($p^{n+1/2}$) and temperature ($T^{n+1/2}$) fields in the first time step, Eqs. (16)-(18), respectively:

$$v_i^{n+1/2} = v_i^n - \mathbf{M}_{DV}^{-1}\{S_i\} \qquad (i = 1,2 \text{ and } 3) \tag{16}$$

$$P^{n+1/2} = \mathbf{M}_{DP}^{-1} \cdot \tilde{\mathbf{M}} \cdot P^n - \mathbf{M}_{DP}^{-1}\{T_C\} \tag{17}$$

$$T^{n+1/2} = T^n - \mathbf{M}_{DT}^{-1}\{S_T\} \tag{18}$$

(4) Impose the boundary conditions of velocity ($v_i^{n+1/2}$), pressure ($p^{n+1/2}$) and temperature ($T^{n+1/2}$) fields;
(5) Form the vectors $\{R_i\}$, $\{Q\}$ and $\{R_T\}$, Eq. (19)-(21), related to the velocity, pressure and temperature fields in the second time step:

$$\{R_i\} = \Delta t\left\{\mathbf{A}_j(v_i)^{n+1/2} + \mathbf{D}_{ij}(v_j)^n - \mathbf{G}_i P^{n+1/2} + (\mathbf{B}_i T - \mathbf{F}_i)^n\right\} \qquad (i,j = 1,2 \text{ and } 3) \tag{19}$$

$$\{Q\} = \Delta t\left\{\mathbf{G}_j^T(v_j) + \mathbf{K}_j(P)\right\}^{n+1/2} \qquad (j = 1,2 \text{ and } 3) \tag{20}$$

$$\{R_T\} = \Delta t\left\{\mathbf{A}_{jT}(T)^{n+1/2} + \mathbf{D}_{jT}(T)^n - \mathbf{F}_T^n\right\} \qquad (j = 1,2 \text{ and } 3) \tag{21}$$

(6) Calculate the velocity ($v_i^{n+1}$), pressure ($p^{n+1}$) and temperature ($T^{n+1}$) in the second time step:

$$v_i^{n+1} = v_i^n - \mathbf{M}_{DV}^{-1}\{R_i\} \qquad (i = 1,2 \text{ and } 3) \tag{22}$$

$$P^{n+1} = \mathbf{M}_{DP}^{-1} \cdot \tilde{\mathbf{M}} \cdot P^n - \mathbf{M}_{DP}^{-1}\{Q\} \tag{23}$$

$$T^{n+1} = T^n - \mathbf{M}_{DT}^{-1}\{R_T\} \tag{24}$$

(7) Impose the boundary conditions;
(8) If the final time established for the simulation is reached the algorithm is finished, otherwise, return to step (1);
In the above equations, $\mathbf{K}_j$ is the advective matrix of pressure, and the matrix $\tilde{\mathbf{M}}$ is given by Eq. (25):

$$\tilde{\mathbf{M}} = e\mathbf{M}_{DP} + (1-e)\mathbf{M}_P \tag{25}$$

where $e$ is referred to as the selective lumping parameter, which controls the numerical damping and numerical stability. The parameter values are in the range of $0 \leq e \leq 1$. In the present work, it is investigated the influence of this selective parameter in the velocity and temperature fields of transient non-isothermal cavities flows.

### 3.3. Stability Consideration

The two temporal schemes analyzed, EITG and TSE, are of an explicit nature. Then, the solution is conditionally stable, and it is necessary to satisfy the Courant's stability condition. Accordingly, the critical time step is given by:

$$\Delta t \leq \Delta x_i(\min)/(C+V) \tag{26}$$

where $\Delta x_i(\min)$ is the smallest element in the domain, and $V$ is the reference velocity.

## 4. DESCRIPTION OF THE PROBLEM

The analysis of the problem considers non-isothermal flows with $Re_H = 400$, $Ri = 0.1$ and $Pr = 6$ in two- and three dimensional cavities with square cross section, as seen in Fig.1. For two-dimensional simulations, only one element is

considered for the *z*-direction. The sizes for the depth of the cavity in two- and three-dimensional cavities, as well as, the numerical and computational parameters are shown in Tab. 1. The fluid flow in the cavity is generated by the motion of an infinite plate that also represents the top surface (*xz* plane), where the velocity of the plate is taken as the reference velocity for the computation of the Reynolds number. In addition, this surface presents the non-slip and impermeability boundary conditions. In the lateral (*yz* planes) and lower (*xz* plane) surfaces, the dimensionless velocities are prescribed as null ($v_1^* = v_2^* = v_3^* = 0$). The others surfaces are treated as symmetric. For the thermal field, the heating of the fluid is a result of imposing a dimensionless temperature of $T^* = 1$ on the upper surface, representing a stable stratification case, and the temperature of the lower surface is prescribed as $T^* = 0$. The lateral (plane *yz*) and frontal (plane *xy*) surfaces are treated as adiabatic. The dimensionless terms (coordinates, velocity, temperature and time) represented by the superscript $^*$, are defined by Eq. (27):

$$x_i^* = \frac{x_i}{H} \qquad v_i^* = \frac{v_i}{H} \qquad T^* = \frac{(T - T_{\inf})}{(T_{\sup} - T_{\inf})} \qquad t^* = \frac{t v_{1\max}}{H} \qquad (i = 1,2 \text{ and } 3) \tag{27}$$

where $H$ is the height of the cavity (the characteristic length used in the computation of Reynolds number), $v_{1\max}$ is the sliding velocity of the top surface and $T_{\sup}$ and $T_{\inf}$ are the largest and smallest temperatures in the cavity.

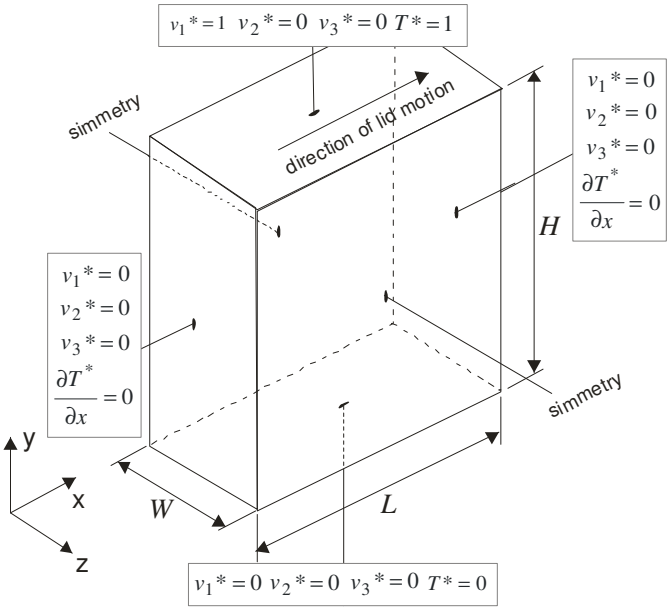


Figure 1. Three-dimensional cavity flow domain and its imposed boundary conditions

For the initial conditions, it is considered that the fluid is still, with null velocities and pressure in the entire domain, and with a stratified temperature field, defined by a linear function along the dimensionless coordinate $y^*$, that is, varying linearly from the temperature on the lower surface to the top surface.

Table 1. Computational and numerical parameters that were adopted in the simulations shown in this work

| Parameter | Two-dimensional flow | Three-dimensional flow |
|---|---|---|
| Cavity domain ($x^*$, $y^*$, $z^*$) | $1 \times 1 \times 1 \times 10^{-2}$ | $1 \times 1 \times 0.50$ |
| Grid ($x^*$, $y^*$, $z^*$) | $100 \times 100 \times 1$ | $100 \times 100 \times 25$ |
| Critical time step (s) | $1.75 \times 10^{-6}$ | $1.75 \times 10^{-6}$ |
| Computational environment | Sun Fire X 2200, AMD Opteron 1.8GHz Dual Core | |

The grid independence for each flow is achieved when the relative deviation between the average profiles of velocity and temperature obtained for two grids are less than 0.1%. For instance, to establish the grid independence, for the two-dimensional case employing both temporal schemes, the following grids were compared: 40×40×1, 60×60×1, 80×80×1, 100×100×1 e 120×120×1. All the results were obtained for an instant of time of $4.40 \times 10^{-2}$ s. Since the boundary conditions are not subjected to random perturbation, the solutions can be deterministically determined.

## 5. RESULTS AND DISCUSSION

Firstly, various selective parameters, $e$, are compared since they are employed in the TSE scheme. The proper choice of this parameter is necessary to avoid numerical instabilities or excessive damping. For this analysis a numerical sensor was placed in the position $x^*$= 0.5 and $y^*$= 0.27 in order to evaluate the time evolution of dimensionless velocity in $x^*$-direction ($v_1^*$) and temperature ($T^*$). In the present study the following selective parameters are evaluated: $e$ = 0.0, 0.7 e 0.95. These values were the same that were adopted in the simulations of Kawahara and Hirano (1983). Figure 2a shows the time evolution of dimensionless velocity in $x^*$-direction. All selective parameters led to few oscillations in the velocity field in the beginning of the process ($t^* \leq 5$). A portion of these oscillations was a result from the abrupt motion of the top surface, which was initially still. Nevertheless, when $e$ = 0.95 is adopted, the velocity field seems to include some numerical instability, since the oscillations are higher for this selective parameter value than for the others. On the contrary, when $e$ = 0.0 led to a slight damping effect, as observed for $t^* \geq 12$. Concerning the temperature fields, the differences between the temperatures for all selective parameters were negligible, as can be seen in Fig. 2b. The best choice of the selective parameter for the present simulations was $e$ = 0.7, which is in accordance with the evaluated by Kawahara and Hirano (1983).

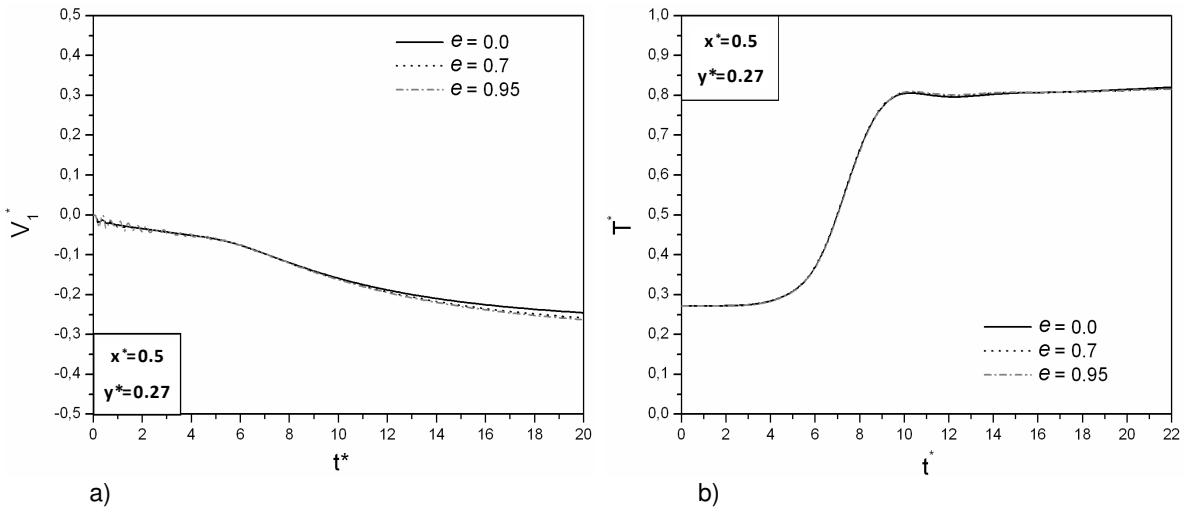


Figure 2. Influence of various selective parameters, $e$ = 0.0, 0.7 and 0.95, in the transient dimensionless fields – a) velocity in $x^*$-direction and b) temperature ($T^*$)

For a quantitative analysis of velocity and temperature fields in the simulation of transient, non-isothermal cavity flows in laminar regime ($Re_H$ = 400, $Ri$ = 0.1 e $Pr$ = 6) using the temporal schemes EITG and TSE, three numerical sensors were placed in the following positions in the cavity: sensor 1 ($x^*$=0.5, $y^*$=0.27), sensor 2 ($x^*$=0.5, $y^*$=0.48) and sensor 3 ($x^*$=0.5, $y^*$=0.93). These positions allow the collecting of numerical data in the lower, intermediate and top regions of the cavity, respectively. The transient velocity and temperature fields obtained from the two temporal schemes are confronted with those of Ji *et al.* (2007). The topologies were also compared and show a very good agreement. For simplification, they will not be presented here. The comparison between the topologies obtained from EITG temporal scheme and those presented by Ji *et al.* (2007) were previously shown in Dos Santos (2007).

Figures 3a and 3b shows the evolution of the velocity in the $x^*$ direction and the temperature fields, respectively, as a function of the time for sensor 1. In Figure 3a, one can verify that the computed velocity fields from the EITG and TSE schemes were in good accordance with those of Ji *et al.* (2007). Nevertheless, slight differences are observed, for example, the velocity fields computed from TSE scheme were more damped than those of Ji *et al.* (2007), which in turn were more damped than of the results of the EITG scheme. Figure 3b presents the behavior of dimensionless temperature as function of time, and shows that all results were in agreement. However, the temperature fields computed from TSE scheme concurred better with the results of Ji *et al.* (2007) than those of EITG scheme. In the worst situation the percentual deviation was approximately 5.6%. In order to investigate the difference between the velocity and temperature fields predicted from EITG and TSE schemes, a simulation of a forced convection heat transfer in cavity flow ($Re_H$ = 400, $Ri$ = 0 and $Pr$ = 6) employing both schemes is performed. The differences in the velocity and temperature fields were negligible. Therefore, the disagreement between velocity and temperature fields predicted from EITG and TSE schemes occurred only when buoyancy terms were present in the simulation, showing that the disagreement between the two schemes was a result of the different treatments for the buoyancy terms.

Figures 4a and 4b show the evolution of dimensionless velocity in $x^*$ direction and the temperature fields ($T^*$), respectively, as a function of the time for sensor 2. For the velocity field, the EITG scheme predicted slightly better results in comparison with the literature than those computed from TSE scheme. However, one observes that in the

evolution of dimensionless temperature fields both schemes, EITG and TSE, showed a very good agreement with those presented by Ji *et al.* (2007).

Figures 5a and 5b show the evolution of dimensionless velocity in $x^*$ direction and the temperature fields, respectively, as a function of time for sensor 3. In Figure 5a, one can observes a very good concordance between the results predicted by both temporal schemes employed and those presented by Ji *et al.* (2007). Concerning the temperature fields, all results showed slight differences, even so, in general they were in good agreement. The results presented by Ji *et al.* (2007) showed an intermediate behavior between the two results computed from TSE and EITG schemes. The TSE results were more damped than from the other solutions.

In general, for all analyzed locations of the cavity, the behavior of velocity and temperature fields predicted from TSE scheme was more damped than those ones obtained from EITG scheme, and the results of Ji *et al.* (2007) showed an intermediate behavior in comparison with those proposed in the present work. In addition, the average temperature fields predicted from the TSE scheme were higher than the EITG ones, showing better concordance with the results of Ji *et al.* (2007).

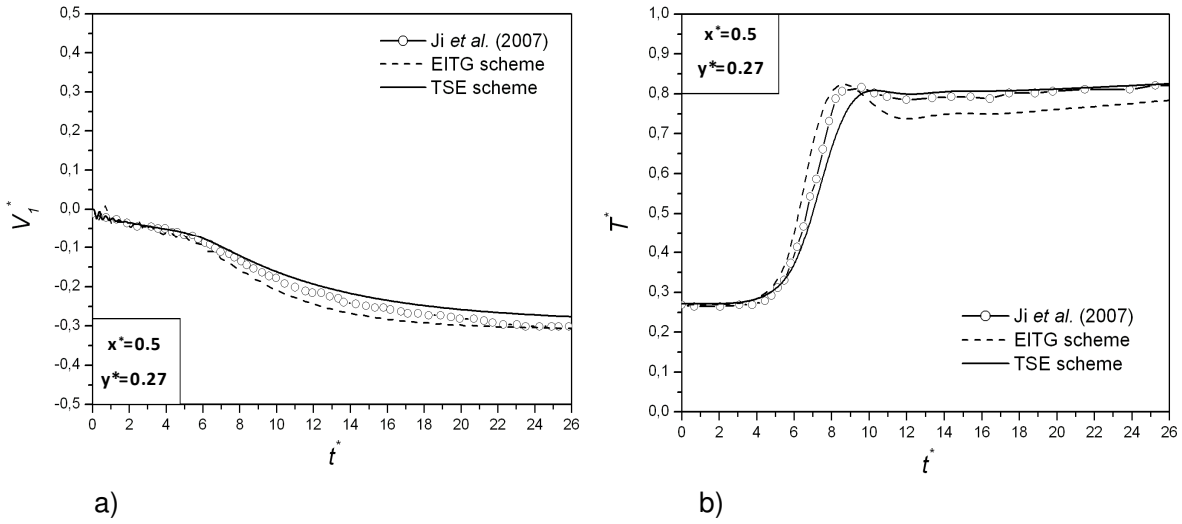


Figure 3. Transient fields for flow with $Re_H = 400$, $Pr = 6$ and $Ri = 0.1$ in sensor 1 ($x^* = 0.5$, $y^* = 0.27$) – a) velocity field and b) temperature field

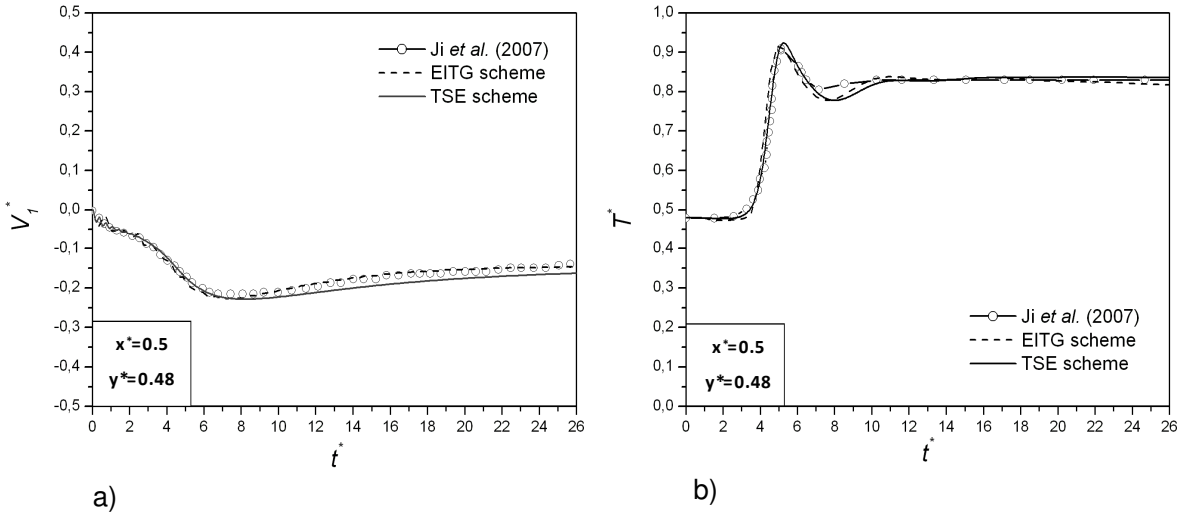


Figure 4. Transient fields for flow with $Re_H = 400$, $Pr = 6$ and $Ri = 0.1$ in sensor 2 ($x^* = 0.5$, $y^* = 0.48$) – a) velocity field and b) temperature field

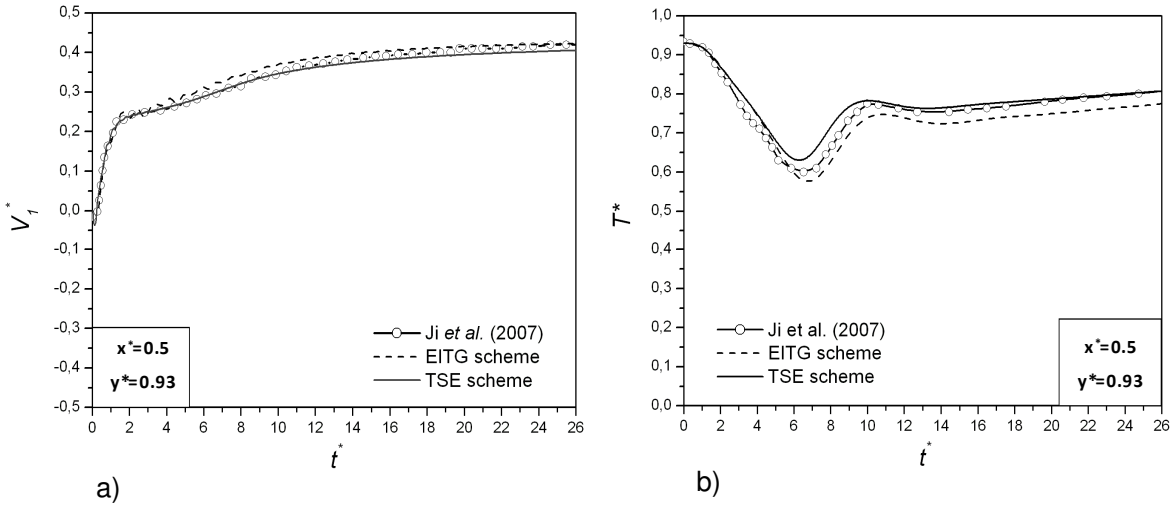


Figure 5. Transient fields for flow with $Re_H = 400$, $Pr = 6$ and $Ri = 0.1$ in sensor 3 ($x^* = 0.5$, $y^* = 0.93$) – a) velocity field and b) temperature field

It is also of interest to investigate the CPU time required in the simulations of non-isothermal cavity flow from the two temporal schemes employed in the present work, EITG and TSE. In order to reliably evaluate the CPU time, the simulations were performed without external influences, that is, the simulations were done using full memory capability. The time processing comparative tests were performed in dual-core Intel processors with 2.67 GHz and memory of 2GB.

Figure 6 presents the time processing required from the employment of EITG and TSE schemes. For all simulations, with many different grids, the time step used is $1.75\times10^{-6}$ s and a final time of $8.75\times10^{-3}$ s. As can be seen, the time processing required from the simulations performed with TSE scheme is significantly lower than those performed with EITG scheme, approximately 8 times. This large difference makes the TSE scheme more suitable than EITG in the simulations of non-isothermal transient flows, especially when more complex flows are studied, such as three-dimensional and turbulent flows. Figure 6 also shows that the increase of CPU time as function of grid number elements did not show a linear behavior. This fact is perhaps linked to the memory manipulation, especially cache memory.

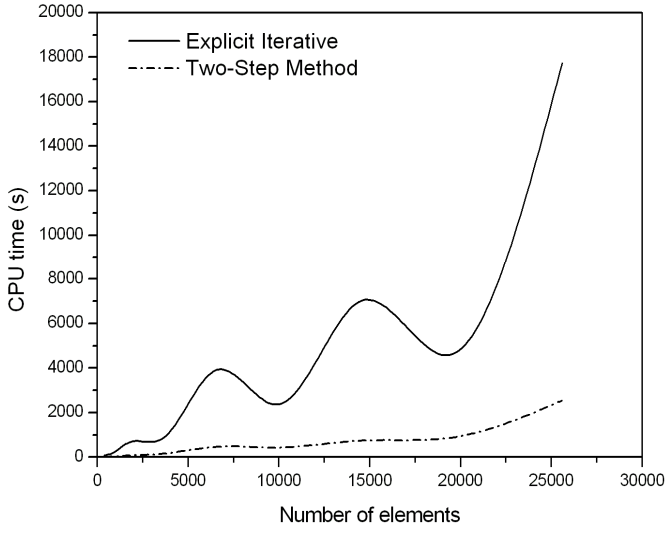


Figure 6. CPU time employing EITG and TSE temporal schemes

For the simulation of three-dimensional cavity flows, it is employed only the TSE scheme, since it predicted well the velocity and temperature fields, and significantly improved the computational performance of the code. The dimensionless parameters employed in a 3D simulations were the same of the 2D simulations, $Re_H = 400$, $Pr = 6$ and $Ri = 0.1$.

Figure 7 presents the time evolution of the temperature. Figures 7a-f show the topologies of the temperature fields for the following dimensionless times: $t^* = 3.0$, $t^* = 9.0$, $t^* = 15.0$, $t^* = 21.0$, $t^* = 30.0$, $t^* = 189.8$, respectively. In the

beginning of the flow, Fig 7a, one observes the start of the formation of Kelvin-Helmholtz eddies, also verified for the two-dimensional simulation. This spiral shaped vortices are generated by the difference of velocities in the cavity that is imposed by the sliding top surface. Moreover, at this instant of time, it was noted a quasi two-dimensional behavior of the flow. As time advances, the first three-dimensional structures emerged, Fig. 7b. At this point the isotherms in the lower portion of left surface were deformed due to a mixing layer in the transverse direction, since the front and back surfaces are at different velocities. Afterwards, it was observed a displacement of the hot mass of fluid from upper surface towards the lower surface, and from the back towards the front surface. Additionally, this heated mass of fluid was mixed in the main vortex, Fig. 7c – e. This process went on until the steady state was reached. Figure 7f illustrates the topology of thermal field when the flow tended to the steady state.

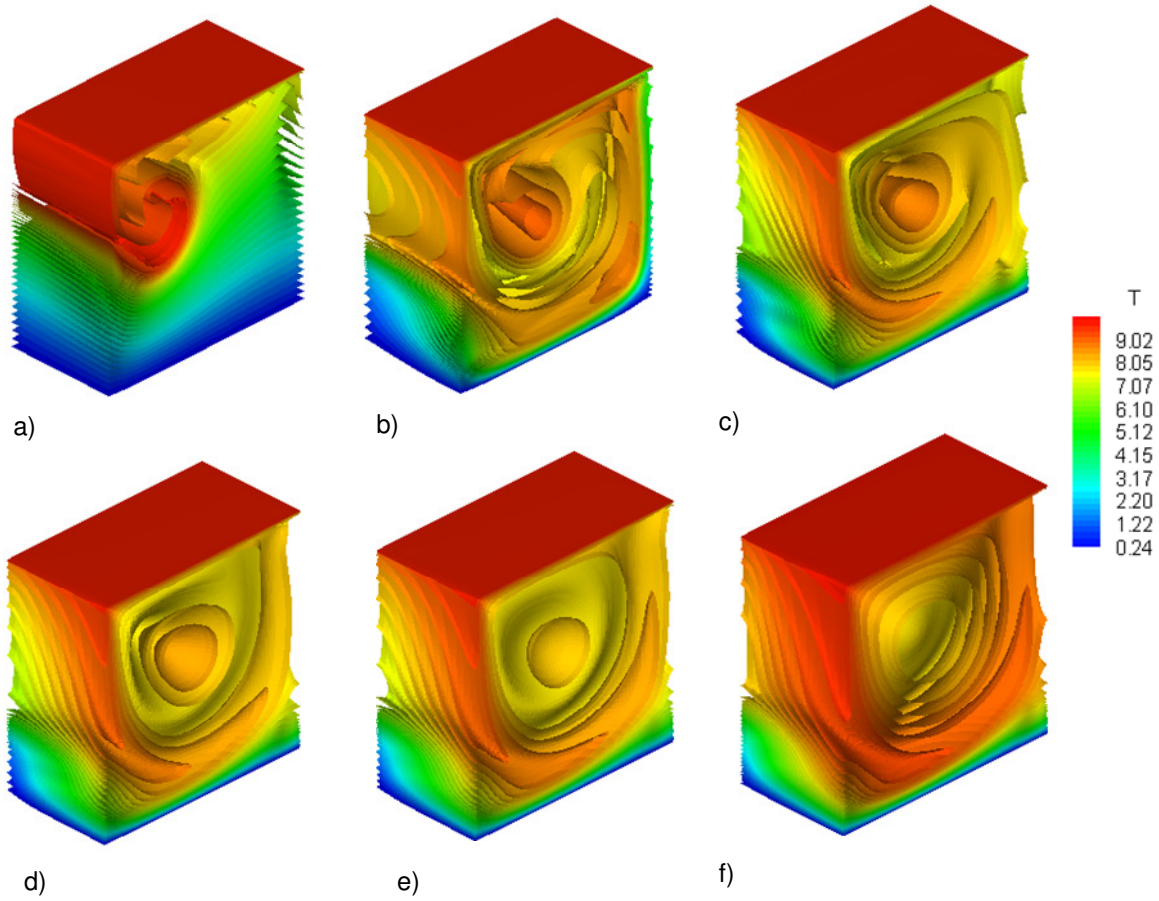


Figure 7. Topologies of the temperature fields for different instants of time for $Re_H = 400$, $Pr = 6$ e $Ri = 0.1$: a) $t^* = 3.0$, b) $t^* = 9.0$, c) $t^* = 15.0$, d) $t^* = 21.0$, e) $t^* = 30.0$ and f) $t^* = 189.8$

## 6. CONCLUSIONS

This work presented a numerical study of transient, laminar cavity flows with mixed convection heat transfer in both two- and three-dimensional domains. It was analyzed the fluid dynamic and thermal behavior of these flows employing two different temporal schemes: Explicit Iterative of Taylor-Galerkin (EITG) and Two Step Explicit (TSE). The numerical solution is based in the finite element method code with hexahedral element and using reduced integration of element matrices.

Various selective parameters were tested in the TSE scheme simulations in order to avoid numerical oscillation or damping. For the present simulations, the parameter $e = 0.7$ led to the best results, showing agreement with the selective parameter suggested in Kawahara and Hirano (1983). Simulations for transient non-isothermal flows for $Re_H = 400$, $Pr = 6$ and $Ri = 0.1$ were obtained in this work from the two different temporal schemes studied: EITG and TSE. The velocity and temperature fields obtained from both schemes were confronted with those of Ji *et al.* (2007), the results agreed within 6%. In addition, the velocity and temperature fields computed from TSE were more damped than those of EITG, even so, the temperature field computed from TSE scheme was in better concordance with the literature one than that predicted from EITG scheme. The disagreement between the two schemes is a result of the different treatment of the buoyancy terms. Concerning the CPU time requisition, the simulations performed with TSE scheme were 8 times, in average, faster than those computed with EITG scheme. Moreover, a three-dimensional simulation for $Re_H = 400$, $Pr =$

6 and $Ri$ = 0.1 was performed from TSE temporal scheme. The methodology proved successful to capture not only typical structures of two-dimensional flows, as Kelvin-Helmholtz vortices, but also three-dimensional ones, as transverse mixture layers similar to Taylor-Göertler vortices.

## 7. ACKNOWLEDGEMENTS

The first and second authors thank CAPES and CNPQ by their doctorate and master scholarship; F. H. R. França thanks CNPq for research grant 304535/2007-9. The authors also thank the National Center of Supercomputation (CESUP-RS) for the technical support.

## 8. REFERENCES

Braun, A.L., 2007, "Numerical simulation in wind engineering including efects of fluid-structure interaction (in Portuguese)", Dsc. Thesis, Universidade Federal do Rio Grande do Sul, Porto Alegre, Brasil.

Braun, A.L., Awruch, A.M., 2003, "Numerical simulation of the wind action on a long-span bridge deck", Journal of the Brazilian Society of Mechanical Science and Engineering, Vol. XXV, nº4, pp. 352-363.

Chorin, A.J., 1967, "A numerical method for solving incompressible viscous flow problems", Journal of Computational Physics, Vol. 2, pp. 12-26.

Dos Santos, E.D., 2007, " Analysis of Non-isothermal, incompressible flows, using large eddy simulations and finite element method (in portugueses)", Msc. Dissertation Thesis, Universidade Federal do Rio Grande do Sul, Porto Alegre, Brasil.

Dos Santos, E.D., Petry, A.P., Xavier, C.M., 2007, "Large eddy simulation of incompressible, three-dimensional and non-isothermal flows in cavities and channels" (In Portuguese), 8º Congreso Iberoamericano de Ingenieria Mecánica, Cusco, Perú, < http://www.pucp.edu.pe/congreso/cibim8/pdf/16/16-36.pdf >

Iwatsu, R., Hyun, J.M., 2007, "Three-dimensional driven-cavity flows with a vertical temperature gradient", International Journal of Heat and Mass Transfer, Vol. 38, pp. 3319-3328.

Ji, T. H., Kim, S.Y., Hyun, J.M., 2007, "Transient mixed convection in an enclosure driven by sliding lid", Heat and Mass Transfer, Vol. 43, pp. 629-638.

Kawahara, M., Hirano, H., 1983, "A finite element method for high Reynolds number viscous fluid flow using Two Step explicit scheme", International Journal for Numerical Methods in Fluids, Vol. 3, pp. 137-163.

Petry, A.P., 1993, "Numerical analysis of fluid-structure interaction by the finite element method (in Portuguese)", Msc. Dissertation Thesis, Universidade Federal do Rio Grande do Sul, Porto Alegre, Brasil.

Petry, A.P, Awruch, A.M., 2006, "Large eddy simulation of three-dimensional turbulent flows by the finite element method", Journal of the Brazilian Society of Mechanical Sciences and Engineering, Vol. 28, pp. 224-232.

Piccoli, G.L., Dos Santos, E.D., Petry, A.P., 2008, "High-Performance programing for computational wind engineering applications", 12th Brazilian Congress of Thermal Engineering and Sciences, Belo Horizonte, Brasil.

Popiolek, T.L., Awruch, A.M., Teixeira, P.R.F., 2006. "Finite element analysis of laminar and turbulent flows using LES and subgrid-scale models", Applied Mathematical Modelling, Vol. 30, pp. 177-199.

Reddy, J.N., Gartling, D.K., 1994, "The finite element method in heat transfer and fluid dynamics", CRC, Boca Raton, Florida, USA, 390 p.

Teixeira, P.R.F., Awruch, A.M., 2001, "Three-dimensional simulation of high compressible flows using a multi-time-step integration technique with subcycles", Applied Mathematical Modelling, Vol. 25, pp. 613-627.

Wang, L., Dong, Y., Lu, X., 2005, "An investigation of turbulent open channel flow with heat transfer by large eddy simulation", Computers & Fluids, Vol. 34, pp. 23-47.

Zienkiewicz, O.C., Taylor, R.L., 2000, "The finite element method – volume 3: fluid dynamics", Butterworth-Heinemann, New York, USA.

## 9. RESPONSIBILITY NOTICE

The author(s) is (are) the only responsible for the printed material included in this paper.